

# Parallel Approximate Ideal Restriction Multigrid for Solving the $S_N$ Transport Equations

Joshua Hanophy,<sup>\*,a</sup> Ben S. Southworth,<sup>b</sup> Ruipeng Li,<sup>c</sup> Jim Morel,<sup>a</sup> and Tom  
Manteuffel<sup>b</sup>

<sup>a</sup>*Texas A&M University, Department of Nuclear Engineering  
210 Animal Industries, College Station, TX 77843*

<sup>b</sup>*University of Colorado at Boulder, Department of Applied Mathematics  
Engineering Center ECOT 225, 526 UCB, Boulder, CO 80309*

<sup>c</sup>*Lawrence Livermore National Lab  
7000 East Avenue, Livermore, CA 94550*

\*Email: [jthano@tamu.edu](mailto:jthano@tamu.edu)

Number of pages: 26  
Number of tables: 5  
Number of figures: 13

### Abstract

The computational kernel in solving the  $S_N$  transport equations is the parallel sweep, which corresponds to directly inverting a block lower triangular linear system that arises in discretizations of the linear transport equation. Existing parallel sweep algorithms are fairly efficient on structured grids, but still have polynomial scaling,  $P^{1/d}$  for  $d$  dimensions and  $P$  processors. Moreover, an efficient scalable parallel sweep algorithm for use on general unstructured meshes remains elusive. Recently, a classical algebraic multigrid (AMG) method based on approximate ideal restriction (AIR) was developed for nonsymmetric matrices and shown to be an effective solver for linear transport. Motivated by the superior scalability of AMG methods (logarithmic in  $P$ ) as well as the simplicity with which AMG methods can be used in most situations, including on arbitrary unstructured meshes, this paper investigates the use of parallel AIR (pAIR) for solving the  $S_N$  transport equations with source iteration in place of parallel sweeps. Results presented in this paper show that pAIR is a robust and scalable solver. Although sweeps are still shown to be much faster than pAIR on a structured mesh of a unit cube, pAIR is shown to perform similarly on both a structured and unstructured mesh, and offers a new, simple, black box alternative to parallel transport sweeps.

**Keywords** — transport, multigrid, sweep

## I. INTRODUCTION

Consider the monoenergetic transport equation with spatially dependent isotropic cross sections,  $\sigma_s$  and  $\sigma_t$ , and an isotropic source,  $q$ ,

$$\vec{\Omega} \cdot \nabla \psi(\vec{r}, \vec{\Omega}) + \sigma_t \psi(\vec{r}, \vec{\Omega}) = \frac{\sigma_s}{4\pi} \phi(\vec{r}) + \frac{q}{4\pi}, \quad (1)$$

where  $\psi$  is the angular flux and  $\phi$  is the scalar flux equal to the integral of the angular flux over all directions,  $\phi = \int_{4\pi} \psi d\Omega$ . The  $S_N$  equations are derived by first selecting a quadrature set to approximate the integral over all directions and then defining the scalar flux as

$$\begin{aligned} \phi(\vec{r}) &= \sum_{m=1}^M w_m \psi_m(\vec{r}), \\ \psi_m(\vec{r}) &= \psi(\vec{r}, \vec{\Omega}_m). \end{aligned} \quad (2)$$

Evaluating Equation 1 at the quadrature points results in  $M$  coupled equations that are discrete in direction,

$$\vec{\Omega} \cdot \nabla \psi_m(\vec{r}) + \sigma_t \psi_m(\vec{r}) = \frac{\sigma_s}{4\pi} \phi(\vec{r}) + \frac{q}{4\pi}. \quad (3)$$

In principle, Equation (3) could be discretized in space and solved for all  $\{\psi_m\}$ ; however, the resulting linear system would have  $M/h^3$  degrees of freedom (DOFs), where  $M$  is the total number of directions and  $h$  the mesh spacing, which is too large for practical calculations. A common technique to avoid the large coupled system is to solve these equations iteratively, which is referred to as ‘‘source iteration.’’ Source iteration involves lagging the scalar flux, first updating  $\{\psi_m\}$  for the  $M$  independent angles and proceeding to update the scalar flux, that is solve

$$\vec{\Omega}_m \cdot \nabla \psi_m^{n+1}(\vec{r}) + \sigma_t \psi_m^{n+1}(\vec{r}) = \frac{\sigma_s}{4\pi} \phi^n(\vec{r}) + \frac{q}{4\pi} \quad (4)$$

for  $m = 1, \dots, M$ , and form  $\phi^{n+1}$  based on  $\{\psi_m^{n+1}\}$  from (2), where  $n$  is the iteration index.

The upwind discontinuous Galerkin (DG) discretization is investigated exclusively in this paper [1]. The upwind DG weak formulation for the steady state transport equation for each direction  $\Omega$  takes the weak form

$$\begin{aligned} - \sum_{T \in T_h} (u_h^{n+1}, \Omega \cdot \nabla v_h) - \sum_{F \in F_h^i} \langle \cdot, \cdot \rangle_F + \sum_{T \in T_h} (\sigma_t u_h^{n+1}, v_h) + \\ \langle u_h^{n+1}, v_h \Omega \cdot \mathbf{n} \rangle_{\Gamma^+} = - \langle g, v_h \Omega \cdot \mathbf{n} \rangle_{\Gamma^-} + \sum_{T \in T_h} (q_{total}^n, v_h). \end{aligned} \quad (5)$$

Here,  $n$  and  $n + 1$  are iteration indices,  $(\cdot, \cdot)_T$  are inner products over the volume, and  $\langle \cdot, \cdot \rangle_T$  are inner products over the faces. The jump term is given by  $[v_h \mathbf{n}] = v_h \mathbf{n}^+ - v_h \mathbf{n}^-$ , where  $+$  and  $-$  superscripts refer to the upwind and downwind faces respectively,  $q_{total}$  is the total source term, including a volumetric source and scattering source, and with the scalar flux lagged as shown in Equation 4. Last,  $\Gamma^-$  is the inflow boundary,  $\Gamma^+$  is the outflow boundary, and  $g$  is a boundary source on the inflow boundary.

For simplicity, only isoparametric multilinear quadrilateral and hexahedral elements are considered in this paper. However, the multigrid solver used here has shown to be effective on higher order elements [2, 3] and curvilinear meshes [4] as well, and results presented here are expected to extend to arbitrary mesh and element order.

### I.A. Solution of the Transport Equation by Sweeping

Upwind discretizations (such as upwind DG) are typically used to discretize Equation 3 for each  $m$ , because the resulting matrix is logically block lower triangular. A forward solve, or “sweep” in transport literature, can then be used to directly invert the matrix. Although a forward solve is a sequential process, parallel algorithms have been developed to perform a forward solve for the sparse discretizations resulting from a fixed angular flux direction. One popular method for parallel sweeping is the KBA method proposed by Koch, Baker, and Alcouffe [5]. For efficiency, this method relies on a specific decomposition of the spatial cells among the processors being used to solve the problem, as well as an ordering of cells for a given angle such that the matrix is lower triangular in that ordering. On a structured mesh, the sweep ordering of cells in a uniform mesh is trivial to determine, but on an unstructured mesh determining a good ordering is a difficult problem (for example, see [6]).

The parallel sweeping algorithm is not particularly efficient for one direction. However, parallel efficiency of such algorithms is improved by solving multiple directions at a time. When multiple directions are solved simultaneously, a scheduling algorithm is generally required to handle the situation where solution fronts for different angular flux directions collide. This situation was analyzed and a provably optimal scheduling algorithm for uniform meshes developed in [7, 8]. The number of communication stages for such algorithms on a uniform mesh is given by  $\mathcal{O}(M + dP^{1/d})$ , for  $M$  angles,  $P$  processors, and a  $d$ -dimensional problem [7]. For a large number of angles  $M$ , the  $dP^{1/d}$  term can be masked by  $M$ . However, for problems with a small to moderate number of angles, or a very large number of processors,  $dP^{1/d}$  is suboptimal parallel scaling. Implementing an efficient parallel sweep on unstructured meshes is more complicated and remains an area of active research. A review of developments towards efficient parallel sweeps on unstructured meshes is given in [6], but it should be noted that asymptotic complexity is at very best equivalent to that on uniform meshes.

In general, solution of the transport equation requires extensive computing time, up to 90% of wallclock time in large multiphysics simulations. As increasing numbers of processors are available for computation, it is desirable to have an alternative to parallel sweeps with parallel complexity logarithmic in  $P$  rather than polynomial in  $P$ , as well as black-box sweeping capabilities that are robust and independent of meshing and discretization.

### I.B. Use of Algebraic Multigrid (AMG)

This paper considers the use of an algebraic multigrid (AMG) method in place of traditional parallel sweeping, motivated by two factors. First, AMG methods have better optimal scalability than parallel sweeping algorithms, and second, AMG methods can be easily used in a black box manner and do not require specialized domain partitioning. AMG methods are widely used to solve linear systems arising from the discretization of elliptic and parabolic partial differential equations. Ideally, AMG scales linearly with the problem size in floating point operations, and communication cost for parallel AMG scale logarithmically with the number of processors [9]. In an optimal setting, the time to solution of parallel AMG scales like  $\log(P)$ , for  $P$  processors. In practice, factors such as growth of the convergence factor, growth of problem size, and coarse-grid fill in can lead to scaling  $\log^m(P)$  for  $m \geq 1$ . Nevertheless, for reasonable  $m$ , AMG scalability is still asymptotically better than the scaling of transport sweeps,  $dP^{1/d}$ . Recently, a classical AMG method based on an approximate ideal restriction (AIR) was developed for nonsymmetric matrices. AIR has shown to be effective for solving linear systems arising from upwind discontinuous Galerkin (DG) finite element discretizations of advection-diffusion problems, including the hyperbolic limit of pure advection [2, 3]. A parallel version of AIR (pAIR) is now available in the *hypr* library, and this paper investigates the performance of pAIR for solving the  $S_N$  transport equations.

The AIR algorithm and supporting theory are developed in [2] and [3]. Briefly, AIR is a

Petrov-Galerkin AMG method based on the construction of an approximation to a certain ideal restriction operator. The ideal restriction operator exactly removes error modes from the coarse grid that are not in the range of interpolation, or, equivalently, provides an exact correction at coarse-grid points. Such a restriction operator separates the coarse-grid problem from the fine-grid problem, so solving  $A\mathbf{x} = \mathbf{b}$  is reduced to solving two smaller problems. AIR approximates the ideal restriction operator and is thus an approximate reduction-based AMG method. AIR is coupled with a simple interpolation, where coarse-grid points are interpolated by value to the fine grid, and several relaxations over F-points on the fine grid then complement the correction to C-points provided by AIR. Two methods were developed in [2, 3] for computing  $R$ , the local approximate ideal restriction ( $\ell$ AIR) and a method based on the use of a finite Neumann expansion ( $n$ AIR), both of which are examined in this paper. For more details on AIR, please see [2, 3].

### I.C. Sweeping with pAIR

This paper studies the performance of pAIR in  $S_N$  transport simulations, replacing a traditional sweep in source iteration with a pAIR solve for each angle. Section II examines the performance of pAIR on different problems and meshes and compares different parallel relaxation routines. One unique aspect of pAIR over a traditional sweep is that the user has flexibility in how accurately the system is solved. In Section III, a short algebraic analysis followed by numerical tests indicate that only a few pAIR iterations are necessary to reach discretization accuracy. Weak scaling is then discussed in Section IV, and angular parallelism introduced in Section V, where multiple MPI groups store an entire copy of the spatial mesh, and each group solves a subset of the angles, which reduces the total time to solution by 30–50%. Finally, weak scaling and a comparison with traditional sweeps is presented in Section VI

pAIR has been implemented in the publicly available *hypr* library (<https://github.com/hypr-space/hypr>) [10], which is used exclusively in this paper. The program created to solve the  $S_N$  equations relies on the deal.II finite element library [11]. For domain decomposition and manipulation of a fully distributed mesh, deal.II relies on the p4est library [12] and for fully distributed matrices and vectors, deal.II is used with the Trilinos library [13]. The Trilinos ifpack package [14] is used to interface with *hypr*. Note that the linear systems investigated in this paper have a natural block-diagonal structure. For the two-dimensional quadrilateral and three-dimensional hexahedral multi-linear elements, block sizes are four and eight respectively. In principle the block structure can be accounted for directly by the pAIR algorithm (as discussed in [2] and [3]). However, the parallel matrix structures used in the software do not contain block information, so matrices are instead scaled by their block inverse, resulting in a logically lower triangular matrix with a unit diagonal.

## II. PAIR PERFORMANCE FOR TRANSPORT

AIR has proven an effective solver for steady state advection through a medium with discontinuities in the total cross section, using both a uniform mesh and an unstructured mesh [3]. In the works developing the AIR algorithm and supporting theory, simple Jacobi relaxation was shown in practice to be effective and some theoretical basis for the effectiveness was provided. For all the problems investigated as part of this paper, Jacobi relaxation is again found to be a robust relaxation scheme. However, the logically lower triangular nature of transport discretizations investigated in this paper allows for potentially more effective relaxation schemes to be implemented, specifically, an on-processor forward solve can be used as a relaxation method, which exactly inverts the principle submatrix stored on processor,

In Section II.A, the performance of pAIR is compared and demonstrated on a variety of meshes and problem types for the two types of relaxation. Then, pAIR is compared with only using on-processor relaxation as a preconditioner for GMRES (without AMG) in Section II.B. In

practice a transport sweep is sometimes replaced by an on-processor solve either due to ease of implementation or in an attempt to reduce the total time to solution, particularly on unstructured meshes, where sweeps can be very time consuming. Here, we look at the regimes of total opacity where pAIR is better than an on-processor solve.

## II.A. Assessment of pAIR with Different Meshes and Cross-Section Characteristics

In two dimensions, pAIR is tested on four different meshes, a uniform structured mesh and the three meshes shown in Figure 1. The unstructured mesh was generated by meshing the surface structure shown in Figure 1(e) using the Gmsh mesh generator program. The zmesh shown in Figure 1(b) is logically a structured mesh and meant primarily to test high aspect ratio elements [15]. The meshes are distributed over 540 processors and refined to approximately 70,000 spatial DOFs per processor. A sweep is then performed by solving for 32 directions in an angular quadrature set sequentially. This involves constructing a global FEM matrix for a single direction, solving the linear system, then clearing the matrix and repeating these steps for the next direction. For the tests presented in this section, the linear system is solved to machine precision.

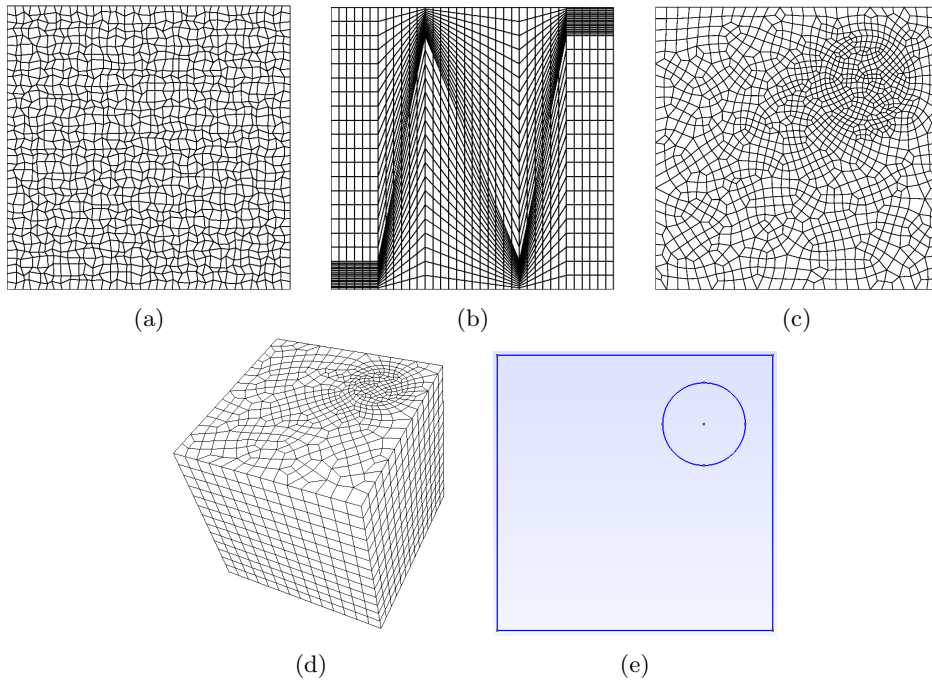


Fig. 1. Four meshes on which pAIR was tested: (a) logically uniform two-dimensional mesh with randomized vertices; (b) two-dimensional zmesh [15]; (c) unstructured two-dimensional mesh; (d) unstructured extruded three-dimensional mesh.

Table I provides the different material compositions tested, with the box and banded configurations depicted in Figure 2. The square domain has a side length 100 cm and a volumetric source of  $1 \frac{n}{cm^2}$ . Inhomogeneous cross sections are implemented such that the cross section is constant within each cell.

Average convergence factors for the homogeneous domain problems are presented in Table II and the average convergence factors for the problems with varied cross sections are presented in Table IV. For the homogeneous problems, the total time for the sweep update to complete are

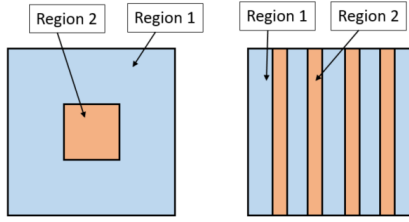


Fig. 2. Schematic of the Box1, Box2, and Banded configuration

TABLE I  
Cross-section Values for the Different Material Configurations Tested

Material Type	Total Cross Section
Box1	Inner Box $0.01 \text{ cm}^{-1}$ , Outer Box $100.0 \text{ cm}^{-1}$
Box2	Inner Box $100.0 \text{ cm}^{-1}$ , Outer Box $0.01 \text{ cm}^{-1}$
Banded	Region 1 $0.01 \text{ cm}^{-1}$ , Region 2 $100.0 \text{ cm}^{-1}$

shown in Table III. Average convergence factors are computed by averaging the convergence factors for each single direction solve.

TABLE II  
Average Convergence Factors for a Full Sweep on the Two-Dimensional Meshes with Homogeneous Cross-Sections

Mesh Type	Relaxation	$\sigma_t = 0.0$	$\sigma_t = 0.01$	$\sigma_t = 1.0$	$\sigma_t = 100.0$
Random Vertices	Jacobi	0.080	0.080	0.071	0.018
	On Proc Solve	0.043	0.044	0.037	0.0013
Uniform	Jacobi	0.036	0.036	0.030	0.0023
	On Proc Solve	0.018	0.018	0.018	1.1e-4
zmsh	Jacobi	0.29	0.29	0.28	0.17
	On Proc Solve	0.052	0.053	0.048	0.010
gmsh	Jacobi	0.22	0.22	0.21	0.13
	On Proc Solve	0.033	0.033	0.028	9.4e-4

TABLE III  
Total Solve Time for a Full Sweep on the Two-Dimensional Meshes with Homogeneous Cross-Sections

Mesh Type	Relaxation	$\sigma_t = 0.0$	$\sigma_t = 0.01$	$\sigma_t = 1.0$	$\sigma_t = 100.0$
Random Vertices	Jacobi	20.5 s	20.2 s	19.1 s	10.8 s
	On Proc Solve	17.4 s	17.2 s	16.9 s	8.63 s
Uniform	Jacobi	11.2 s	11.1 s	11.0 s	5.82 s
	On Proc Solve	11.4 s	11.3 s	10.1 s	4.54 s
zmsh	Jacobi	34.4 s	34.3 s	33.4 s	21.5 s
	On Proc Solve	16.5 s	16.4 s	15.9 s	10.0 s
gmsh	Jacobi	15.7 s	15.5 s	15.7 s	9.70 s
	On Proc Solve	8.27 s	8.25 s	8.16 s	4.02 s

TABLE IV

Average Convergence Factors for a Full Sweep on the Two-Dimensional Meshes with Inhomogeneous Cross-Sections

Mesh Type	Relaxation	box1	box2	banded
Random Vertices	Jacobi	0.079	0.041	0.043
	On Proc Solve	0.042	0.0075	0.0064
Uniform	Jacobi	0.034	0.010	0.0098
	On Proc Solve	0.019	0.0012	9.7e-04
zmsh	Jacobi	0.29	0.19	0.27
	On Proc Solve	0.048	0.010	0.032
gmsh	Jacobi	0.021	0.015	0.018
	On Proc Solve	0.0032	0.0046	0.0066

For all cases tested, simple Jacobi relaxation results in reasonable convergence factors, but the on-processor solve as a relaxation always outperforms Jacobi relaxation. The convergence factors for the unstructured mesh are similar to those of the two logically rectangular grids. For all mesh types investigated, results for the Box1 configuration are very similar to the homogeneous domain test with a cross section of  $100.0 \text{ cm}^{-1}$ . The Box1 configuration has a large outer opaque region and a smaller inner transparent region. The Box2 configuration results are more similar to the homogeneous results with a cross section of  $0.01 \text{ cm}^{-1}$ . An important factor for the solver appears to be the number of optically thin cells, suggesting that results from homogeneous (thin) domains should be a worst-case on heterogeneous domains, consistent with results in [2].

In three dimensions, a uniform structured grid and an unstructured extruded mesh are investigated, with approximately 16,600 spatial DOFs per processor. The unstructured grid is shown in Figure 1. Average convergence factors are presented in Table IV and Table V. Trends similar to those seen in the two-dimensional results are again apparent in the three dimensional results.

TABLE V

Average Convergence Factors for a Full Sweep on the Three-Dimensional Meshes

Mesh Type	Relaxation	$\sigma_t = 0.0$	$\sigma_t = 0.01$	$\sigma_t = 1.0$	$\sigma_t = 100.0$
Uniform	Jacobi	0.14	0.14	0.13	0.034
	On Proc Solve	0.075	0.075	0.069	0.0053
Unstructured	Jacobi	0.17	0.17	0.16	0.043
	On Proc Solve	0.010	0.010	0.094	0.0081

## II.B. Comparison of pAIR with Domain-Wise Block Jacobi

The previous section compared pAIR time to solution when using Jacobi relaxation and an on-processor solve for relaxation. In some cases, the transport sweep in source iteration is actually replaced with the same on-processor solve as an approximate inverse (also known as inexact parallel block Jacobi) [16]. This can be thought of as a block Jacobi iteration, with blocks given by the domain each processor owns. Here, we make a direct comparison between pAIR using an on-processor solve for relaxation, and GMRES preconditioned with an on-processor solve.

Results are based on a simple 2d test problem with homogeneous total cross section  $\sigma_t = C$ , for some constant  $C$ , and direction  $\Omega = (\cos(\theta), \sin(\theta))$ , with  $\theta = 3\pi/16$ . Figure 3 shows the speedup that pAIR provides over GMRES preconditioned with on-processor solve, as a function of  $\sigma_t$ , and for a multiple mesh types, finite-element orders, and local problem sizes. For  $\sigma_t \gg 1$ , so-called “optically thick regimes,” the matrix is already well-conditioned and an on-processor



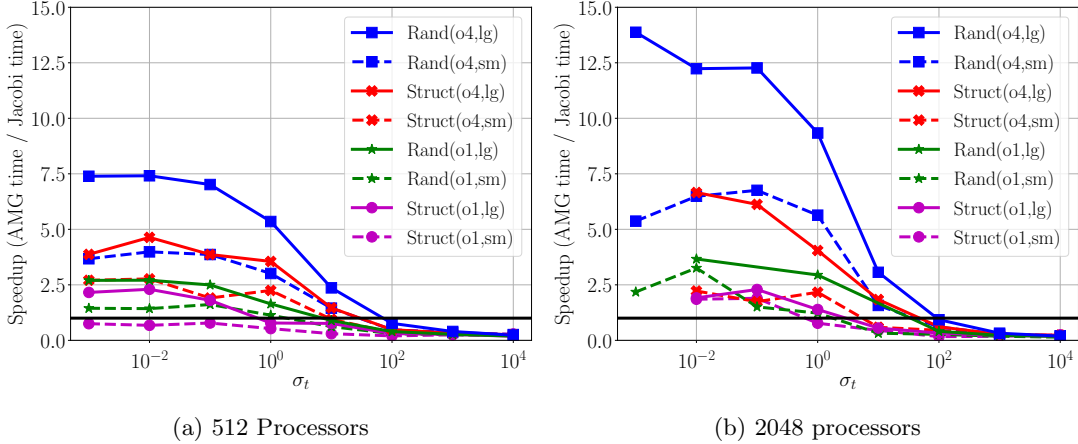


Fig. 3. Comparison of pAIR and GMRES preconditioned with an on-processor solve, as a function of total opacity  $\sigma_t$ , for first- (o1) and fourth-order (o4) finite elements, on structured (struct) and unstructured (rand) meshes, and for a small (sm) and large (lg) on-processor problem size. Local DOFs range from 8,000 for Struct(o1,sm) to 700,000 for Rand(o4,lg).

relaxation converges rapidly without multigrid. For thin regimes,  $\sigma_t < 1$ , however, pAIR leads to as much as a  $14\times$  speedup over GMRES and the on-processor solve. These tests only went up to 2048 processors, but as can be seen, this speedup will continue to grow as more and more processors are used in a weak scaling sense (because block-processor is a Jacobi iteration, and convergence deteriorates as problem size increases),

Note, when an on-processor solve is used in source iteration, typically only one or a few iterations are performed for each source iteration (that is, it is not applied until convergence). However, if there are thin regions in the domain, convergence of the larger source iteration will likely be more-or-less defined by convergence of the block Jacobi algorithm on the thin regions (where convergence will be slowest). The following section investigates how accurately systems must be solve by pAIR.

### III. ACCURACY OF SPATIAL SOLVES

A unique aspect of using an iterative method to solve the linear transport equation compared with traditional sweeps (which are an exact solve) is the question as to how accurately each linear system should be solved. In fact, this question has subtle practical implications, and how accurately the systems are solved actually defines the solution that source iteration converges to.

Consider  $M = 3$  angles and one energy group. Then the full discretized set of equations, replacing the scattering integral with a sum over angular quadrature weights  $\{\omega_i\}$  and corresponding spatial discretization  $\{\mathcal{L}_i\}$ , can be written as a block linear system,

$$\begin{bmatrix} \mathcal{L}_1 & & & -\sigma_s I \\ & \mathcal{L}_2 & & -\sigma_s I \\ & & \mathcal{L}_3 & -\sigma_s I \\ \omega_1 I & \omega_2 I & \omega_3 I & -I \end{bmatrix} \begin{bmatrix} \psi_1 \\ \psi_2 \\ \psi_3 \\ \varphi \end{bmatrix} = \begin{bmatrix} q_1 \\ q_2 \\ q_3 \\ 0 \end{bmatrix},$$

where  $\mathcal{L}_i \sim \Omega_i \cdot \nabla + \sigma_t$ . For memory purposes, the standard approach in transport simulation is to eliminate the block diagonal matrix corresponding to the angular flux vectors, and iterate only on the scalar flux  $\varphi$ . This corresponds to a Schur complement problem for the scalar flux,  $\mathcal{S}\varphi = \mathbf{b}$ ,

where

$$\mathcal{S} := I - \begin{bmatrix} \omega_1 I & \omega_2 I & \omega_3 I \end{bmatrix} \begin{bmatrix} \mathcal{L}_1^{-1} & & \\ & \mathcal{L}_2^{-1} & \\ & & \mathcal{L}_3^{-1} \end{bmatrix} \begin{bmatrix} \sigma_s I \\ \sigma_s I \\ \sigma_s I \end{bmatrix} = I - \sum_{i=1}^f \omega_i \sigma_s \mathcal{L}_i^{-1}.$$

Source iteration corresponds to performing Richardson iteration on  $\mathcal{S}\varphi = \mathbf{b}$ ,

$$\varphi^{(i+1)} = \varphi^{(i)} + \mathbf{b} - \mathcal{S}\varphi^{(i)} = \mathbf{b} + \sum_{i=1}^f \omega_i \sigma_s \mathcal{L}_i^{-1} \varphi^{(i)}.$$

For a detailed discussion on transport iterations in a linear algebra framework, see [17, 18].

Note that a transport sweep, that is computing the action of  $\mathcal{L}_i^{-1}$  for  $i = 1, \dots, M$ , is used to compute *the action* of the operator  $\mathcal{S}$ . Now suppose that we do not invert  $\mathcal{L}_i$  exactly and instead apply  $\widehat{\mathcal{L}}_i^{-1}$ , denoting some  $\ell$  iterations of pAIR for  $\mathcal{L}_i$ . This corresponds to applying Richardson iteration to the modified problem  $\widehat{\mathcal{S}}\varphi = \mathbf{b}$ , where  $\widehat{\mathcal{S}} := I - \sum_{i=1}^3 \omega_i \sigma_s \widehat{\mathcal{L}}_i^{-1}$ . Thus in applying approximate inverses  $\widehat{\mathcal{L}}_i^{-1}$ , corresponding to, say, ten pAIR V-cycles, we actually converging Richardson/source iteration to a modified angular flux problem, defined by the approximate inverses.

There is a standard question in finite element discretizations and linear solvers as to how accurately the liner system must be solved to achieve discretization accuracy (that is, the solution to the linear system is sufficiently accurate that solving to increased accuracy does not lead to better approximation of the continuous solution). Although the question is slightly more complicated here due to the approximate  $\widehat{\mathcal{S}}$  discussed above, a similar question arises – how many V-cycles must we apply such that the solution of  $\widehat{\mathcal{S}}\varphi = \mathbf{b}$  is just as good of an approximation to the continuous PDE as the solution of  $\mathcal{S}\varphi = \mathbf{b}$ ? Some insight into this question is provided in Figure 4, which shows the error (from continuous solution) in the computed scalar flux with a fixed number of pAIR iterations, along with the average final pAIR residual. The error is computed based on a method of manufactured solutions (MMS) for a three dimensional cube with side length of 1 cm discretized and a structured grid. The MMS source is provided in the Appendix. Also shown in the figure is the relative residual for the final source iteration.

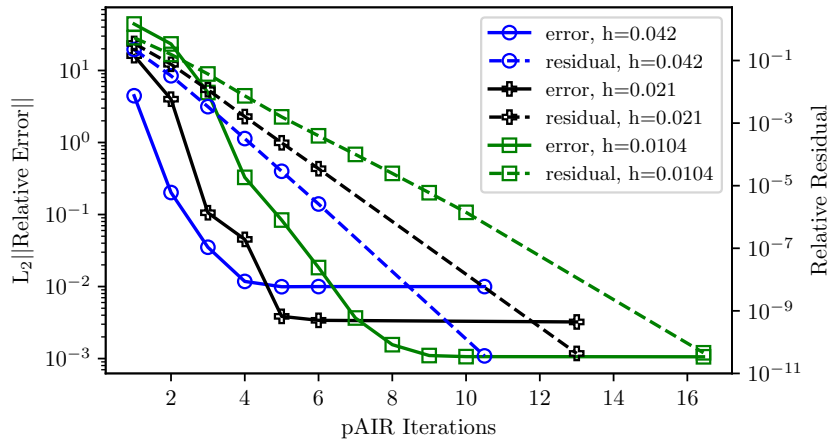


Fig. 4. Comparison of relative error in solution and relative residual versus the number of pAIR iterations. Results from three successively refined meshes are shown where  $h$  is the spacing between vertices.

As expected, as mesh spacing  $h \rightarrow 0$ , the linear systems must be solved to increasingly accurate tolerances, because the solution is also increasingly accurate. However, it is clear that the systems do not need to be solved to machine precision, and only a handful of iterations are necessary for good convergence.

#### IV. WEAK SCALING WITH PARALLELISM IN SPACE

As discussed in Section I.B, for an ideal multigrid method, the total time to solution in a weak scaling test should grow linearly in log-log space, with a slope equal to one when plotted with the logarithm of total problem size (or equivalently the total number of processors). In practice, factors such as growth of the convergence factor and coarse-grid fill in can lead to a slope  $m$ , corresponding to  $\log^m(P)$ , that is greater than one.

Weak scaling results to 4,096 processors for both a three-dimensional uniform grid and unstructured grid are shown in Figure 5. A uniform volumetric source of strength  $1 \frac{n}{cm^3 s}$  was used for both tests. The calculations are performed with a square Chebyshev-Legendre  $S_4$  quadrature set having 32 directions [19]. For the uniform grid, the spatial domain size was fixed at 32,768 DOFs per processor, while the unstructured grid has 50,960 DOFs per processor. Both of these results were generated with distance-2  $\ell$ AIR, pointwise Jacobi relaxation, Falgout coarsening with a strength of connection (SOC) parameter of 0.25, and a strength parameter for  $R$  of  $\epsilon_r = 0.01$  (see Section IV.A.1). In both cases, time to solution grows linear in log-log space for both solve time and setup time, an important initial demonstration of the method’s scalability.

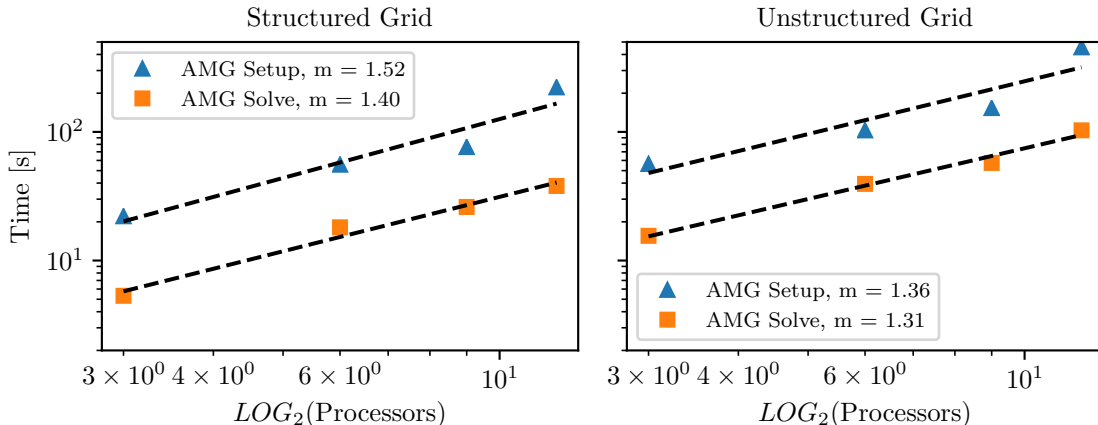


Fig. 5. Scaling results for both a uniform grid and unstructured mesh for distance-2  $\ell$ AIR with no operator filtering. Time reported is that to solve all 32 directions in the angular quadrature set.

##### IV.A. Relevance of Operator Filtering and SOC Parameter

The AMG algorithm includes a number of parameters which affect various aspects of performance. Additionally, pAIR, like other AMG methods, depends on distinct algorithms that accomplish tasks in the overall method, and different algorithms can be used to accomplish the same task. A parameter study is not included as part of this paper, however, some general considerations regarding two important parameters are discussed in the next two sections. These two parameters are particularly relevant to scalability and overall time to solution. They also most markedly affect the total cost of pAIR and should thus be first considered when using pAIR in practice to solve the transport equation.

#### IV.A.1. SOC Parameter for Building $R$

When building the approximate ideal restriction operator  $R$ , each row corresponds to a C-point and has a nonzero sparsity pattern of F-point neighbors. Instead of finding the neighborhood of F-points in the matrix  $A$ , the neighborhood is based on a SOC matrix, where only “strongly” connected F-points are chosen for the sparsity pattern. This increases the sparsity of  $R$  as well as decreasing the cost of computing  $R$ . A coefficient is included in the SOC matrix if it is strongly connected in a classical AMG sense, that is, all columns  $\{j\}$  in row  $i$  such that

$$|a_{ij}| \geq \epsilon_R \max_{i \neq j} (|a_{ij}|) \quad (6)$$

Here a new SOC parameter is introduced,  $\epsilon_R$ , that is generally different than the parameter used for coarsening. Note also that the absolute value of coefficients are used instead of the negative values.

Construction of  $R$  using distance-1 and distance-2  $\ell$ AIR is discussed in Section I.B. In general, convergence factors will improve as the SOC parameter  $\epsilon_R$  is made smaller. However, the time it takes to build  $R$  and apply pAIR will increase as more connections are considered. Figure 6 shows average convergence factors for different  $\epsilon_R$  parameter values for distance-2 and distance-1  $\ell$ AIR respectively, and Figure 7 shows the total pAIR time and setup time for different  $\epsilon_R$  parameter values for distance-2  $\ell$ AIR. Results are presented for both a uniform grid and the unstructured mesh. Although results shown are for a single direction, similar results are seen for each direction in the angular quadrature set investigated.

For both distance-1 and distance-2  $\ell$ AIR, as  $\epsilon_R$  is decreased, the convergence factors decrease. Additionally, there is less convergence factor growth apparent in the weak scaling test for small values of  $\epsilon_R$ . Note that for distance-1  $\ell$ AIR, the convergence factors stop significantly decreasing as  $\epsilon_R$  becomes smaller. This is because after a certain point, most of the distance-1 neighbors are already being considered and decreasing  $\epsilon_R$  does not include any new neighbors. For distance-2  $\ell$ AIR, there are many more possible neighbors and significant differences can be seen in the average convergence factors even between the two relatively small  $\epsilon_R$  values of 0.05 and 0.01.

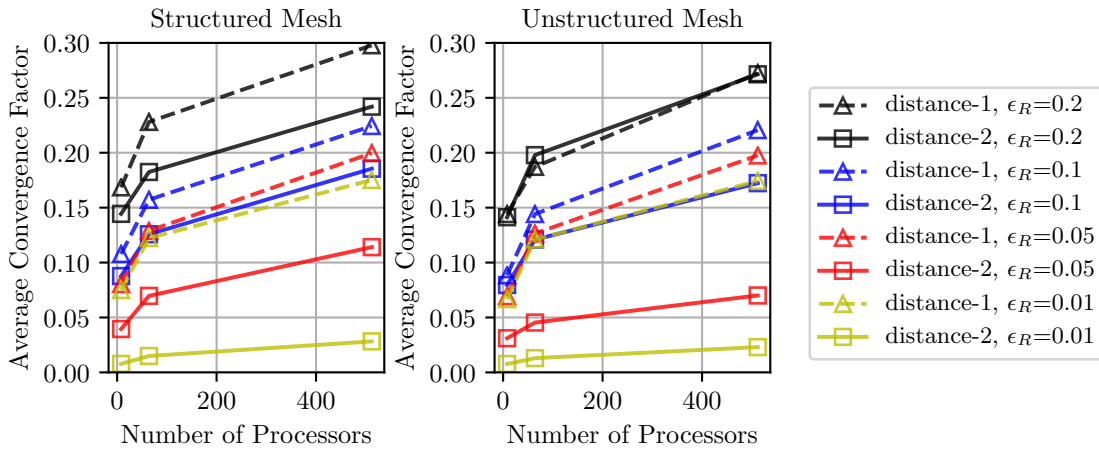


Fig. 6. Average convergence factors for both a uniform mesh and unstructured mesh as  $\epsilon_R$  is made smaller shown for distance-1 and distance-2  $\ell$ AIR.

Interestingly, in direct contrast to convergence factors, total time to solution actually increases as  $\epsilon_R$  decreases, in particular due to an increase in setup time. Note in Figure 7 that the solve time (difference between total and setup) decreases slowly with smaller  $\epsilon_R$ , but the setup time

increase dramatically. Trends are similar for both the uniform mesh and unstructured mesh. The increase in total time for pAIR as  $\epsilon_R$  decreases is more drastic for distance-2  $\ell$ AIR than distance-1  $\ell$ AIR, but trends are similar in both cases. Clearly, for the scaling tests presented Section IV, the largest value of  $\epsilon_R$  that still provides for reasonable convergence should be used.

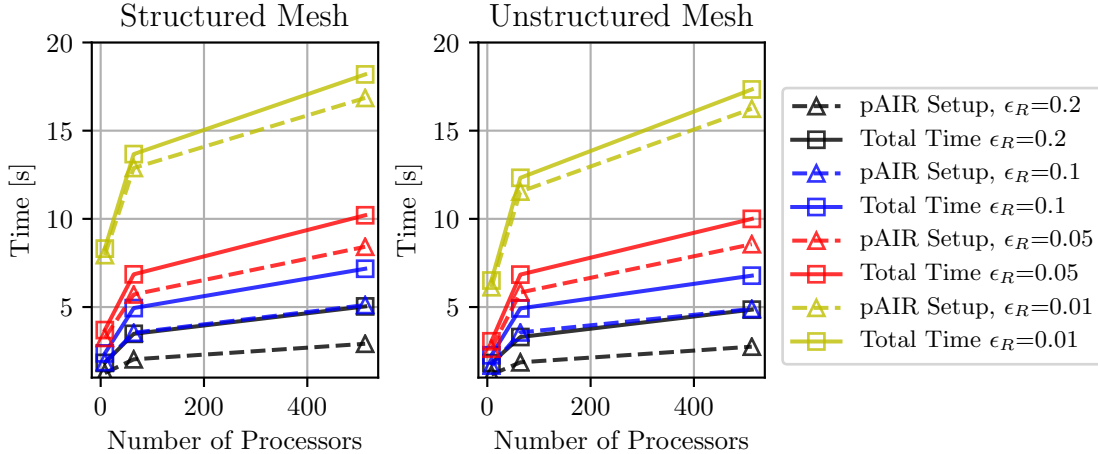


Fig. 7. Comparison of total time to solution with setup time for different  $\epsilon_R$  parameter values.

#### IV.A.2. Stencil Growth and Filtering of $R$

Ideally as problem size increases, the size (in memory) or “complexity” of the AMG hierarchy relative to initial problems size would remain constant, and the average convergence factor would also remain constant. Classical AMG algorithms can exhibit these qualities for some problems such as certain 2-dimensional discretizations of elliptic PDE problems. However, in 3-dimensions, even these PDE problems may exhibit an increasing complexity as the mesh is refined. Complexity can be analyzed in several different ways. One indicator of overall complexity is growth in average stencil size as the mesh is refined. This is equivalent to examining the average number of nonzeros per row for each operator in the AMG hierarchy. For all problems examined in this paper, stencil growth is apparent for a variety of parameter settings.

One strategy for limiting stencil growth is filtering small coefficients from operators. Filtering of matrices in the AIR hierarchy is discussed in [3] where it is pointed out that while filtering of values from symmetric matrices is a sensitive procedure, a system arising from a hyperbolic problem should be less sensitive to filtering. Here we extend that notion to introduce a filtering on  $R$ . This is analogous to the pre- and post-filtering done for interpolation sparsity patterns in the root-node AMG algorithm [20]. Here, a SOC based on  $\epsilon_R$  is used to determine an initial sparsity pattern, then  $R$  is constructed. Once  $R$  is constructed, an analogous SOC as in Equation (6) is applied using a new tolerance,  $\phi_R$ , and non-strong (i.e., weak) entries are eliminated from  $R$ .

Figure 8 shows the significant reduction filtering in  $R$  has on stencil growth for a representative three-dimensional problem, and Figure 9 shows scaling results where small coefficients have been filtered from  $R$  after construction. The pAIR solve is still robust even with large filtering parameter values, and the time to solution and memory consumption drop accordingly.

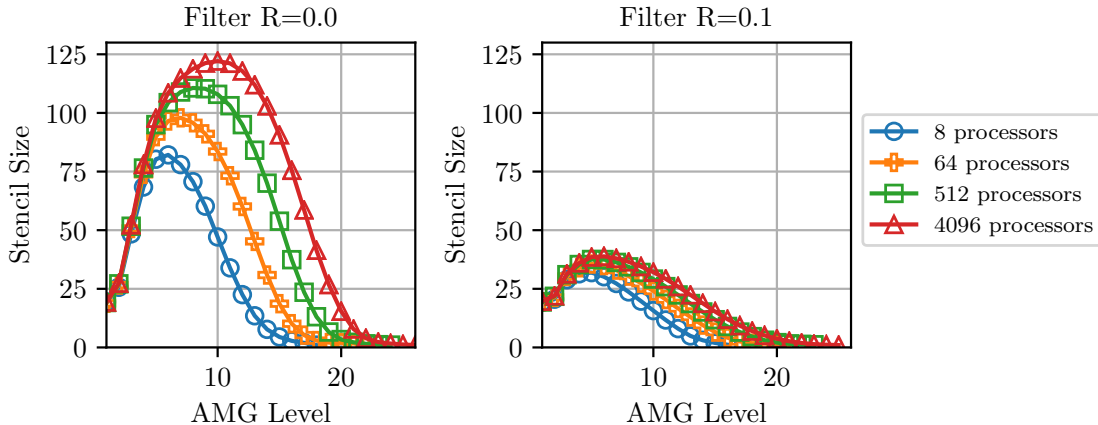


Fig. 8. Comparison of aggressive filtering from  $R$  to no filtering shown with distance-1  $\ell$ AIR for a representative three-dimensional problem

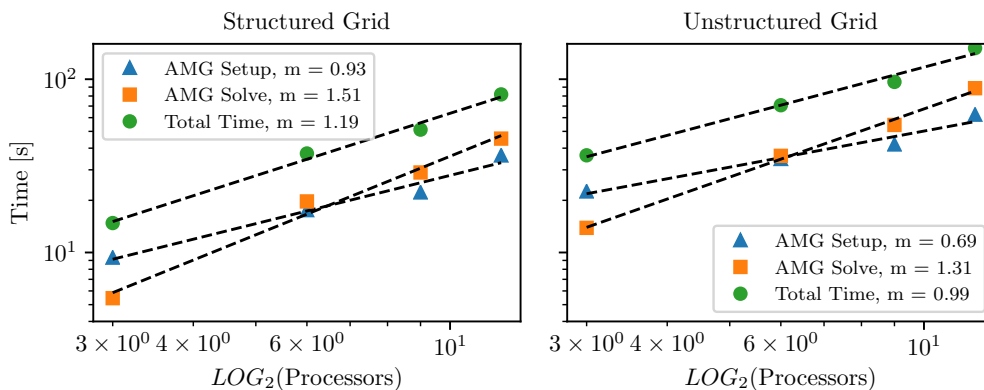


Fig. 9. Scaling results for both a uniform grid and unstructured mesh for distance-1 nAIR with aggressive operator filtering using a filter parameter of  $\phi_R = 0.1$ . Time reported is that to solve all 32 directions in the angular quadrature set.

## V. PARALLEL IN ANGLE AND MINIMIZING COMMUNICATION

In highly parallel environments, whether the transport sweeps are solved using pAIR or a traditional parallel sweep, communication is often the dominant cost, particularly when considering strong scaling. This will be especially true on emerging-type architectures where nodes have GPUs or manycore processors that are particularly fast on threaded, shared-memory-type floating-point operations. To reduce communication cost, we propose including parallelism in the angular and energy domains, in addition to the spatial domain, by storing multiple copies of the spatial discretization. Multiple angles/energies can then be solved for simultaneously, and the overhead communication cost to communicate angular and energy solutions is small compared to the communication cost of spatial solves. Note that analogous ideas have been considered in the context of traditional transport sweeps as well, originally in [21, 22].

This section develops a model for the number of parallel communication stages of pAIR in terms of number of processors, depending on how many copies of the spatial problem are used. In

particular, it is shown that the minimum number of stages of communication is achieved by using the maximum number of spatial meshes that can fit in memory. Although this does not account for computation time, when using pAIR it is a reasonable proxy for computation time as well. When using an on-processor solve for relaxation with pAIR, the larger the portion of spatial domain that is stored on processor, the faster convergence will be, with the obvious limit of a forward (exact) solve in one iteration when the spatial domain is stored on one processor. The performance model is presented in Section V.A, followed by numerical results in Section V.B. For ease of readability, proofs for theoretical results in Section V.A are left to the appendix.

### V.A. A Performance Model

This section develops a simple performance model for stages of communication in a pAIR transport sweep as a function of the number of copies of the spatial discretization. The basic result says that the minimum number of stages of communication is obtained with the maximum number of spatial meshes that can fit in memory.

Let  $N$  denote the total spatial degrees-of-freedom (DOFs),  $M$  the total angular DOFs,  $E$  the total energy DOFs,  $P$  the number of processors, and  $C_P$  the memory capacity of each processor. We are solving for the angular/energy flux,  $\psi_{\ell,\nu}(\mathbf{x})$ , where  $\ell$  denotes the angle,  $\nu$  the energy, and  $\mathbf{x}$  the spatial point. Thus,  $\psi_{\ell,\nu}(\mathbf{x})$  has dimension  $NME$ . We must also account for the memory to store pAIR hierarchies, where one hierarchy is typically equivalent to storing 2–4 copies of the matrix for a single angle. Because memory is a leading constraint in transport simulations, here we only consider the case of storing one hierarchy at a time and, thus, rebuilding a hierarchy for every solve. Following from this discussion, assume that  $P$  processors have sufficient storage for this problem.

**Assumption 1.** *Assume*

$$PC_P \geq NC_T(ME + C_A), \quad (7)$$

where  $C_T$  is a factor that describes the memory required to store each spatial DOF, plus any auxiliary vectors,  $C_A$  a factor that describes the memory to store an AMG hierarchy for a single angle, relative to the storage for all spatial DOFs (should be  $\approx 2-4$ ).

Then, divide the machine into  $K$  equal partitions, each of which includes a full spatial discretization, and distribute the  $ME$  angle and energy DOFs across the  $K$  partitions. That is, each spatial partition addresses  $M_1 = M/K_A$  angles and  $E_1 = E/K_E$  energy groups, where  $K = K_A K_E$ . This implies  $M_1 E_1 = ME/K$ . We further assume that there are not more partitions than angle/energy DOFs.

**Assumption 2.** *Assume that each angle/energy DOF is associated with only one partition, that is,  $K \leq ME$ .*

In the remainder of this section, we assume that all  $M_1 E_1$  angle/energy DOFs associated with a spatial node are stored on the same processor. This simplifies the accumulation of scalar flux and the scattering source.

The size of  $K$  is further restricted by the requirement that the capacity of  $P_x$  processors will accommodate all  $M_1 E_1$  local DOFs and an AMG hierarchy for a single angle/energy. This leads to the following constraint:

**Constraint 1.**

$$P_x C_P \geq NC_T(M_1 E_1 + C_A) \quad \iff \quad K \leq \frac{PC_P - NC_T ME}{C_a NC_T}. \quad (8)$$

Note that Assumption 1 implies Constraint 1 with  $K = 1$ . We can now state the primary results.

**Theorem 1.** Assume Constraint 1 and Assumption 2 hold and that  $pAIR$  scales like  $\mathcal{O}(\log P)$ . Then the optimal  $K$  with respect to minimizing the number of communication stages is given by

$$K_{opt} = \min \left\{ P, ME, \frac{PC_P - NC_T ME}{C_a NC_T} \right\}.$$

**Conjecture 1.** Assume Constraint 1 and Assumption 2 hold and that  $pAIR$  scales like  $\mathcal{O}(\log P)^\alpha$ , for  $\alpha \in (1, 2]$ . Then the optimal  $K$  with respect to minimizing the number of communication stages is given by

$$K_{opt} = \min \left\{ P, ME, \frac{PC_P - NC_T ME}{C_a NC_T} \right\}.$$

Conceptually, these results say that minimizing the number of stages of communication is obtained by using the maximum number of copies of the spatial mesh that fit in memory. Of course this doesn't account for more complex aspects of performance, including computation time, changes in memory access time and message size as the local spatial problem size changes, etc. However, it does suggest that using multiple spatial meshes should improve performance, a result that is consistent with numerical tests in the following subsection.

Note, Conjecture 1 is not proven (or disproven) to hold for all situations, but a partial proof in the Appendix shows that for moderate to large  $P$ , it is very likely to hold, and can be verified for specific values of the above parameters.

## V.B. Parallel in Angle Results

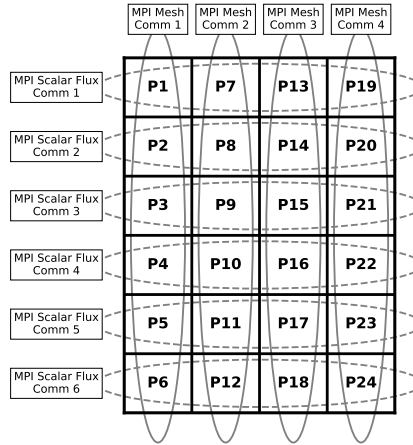


Fig. 10. Schematic showing the grouping of 24 processors into a grid of  $6 \times 4$  MPI communicators. Columns each contain an identical copy of a distributed spatial mesh to solve for angular flux vectors over a subset of directions in the angular discretization. Rows each contain a full angular discretization over a fixed subdomain of the spatial mesh.

Figure 10 provides an example of the parallel in angle implementation on 24 processors, where it is assumed there is sufficient memory to store the spatial mesh and associated variables on six processors. Six MPI groups and associated intra-communicators are thus created and single direction solves are performed on the processors in these groups, each group accounting for the angular flux directions associated with  $1/4$  of the  $M$  directions in the  $S_N$  discretization. To form the scalar flux as a weighted sum over angular flux, these intra-communicators, called MPI



Mesh communicators in Figure 10, must then perform an Allreduce communication, where the contribution from each Mesh communicator to the scalar flux is summed and this sum is made available to all processors. To perform this Allreduce, a second MPI grouping is created, denoted as the Scalar Flux communicators in Figure 10. Note the spatial mesh must be distributed in exactly the same way based on MPI rank in each MPI Mesh communicator. This is easily accomplished with the software libraries used here.

The weak scaling tests using a three-dimensional structured mesh described in Section IV are now repeated for the parallel in space and angle implementation. Three different parallel in angle simulations are performed using two, four, and eight replicated meshes respectively, with an on-processor solve for relaxation. Results from four specific configurations are presented in this section, two using  $\ell$ AIR and two using nAIR, and with two values of filtering for  $R$ . These specific cases are presented because there is significant difference between the D-2  $\ell$ AIR algorithm and the degree-1 nAIR algorithm. Additionally, with heavy operator filtering, stencil growth is minimized along with the overall communication costs. Despite this, significant speed up is seen at 4096 processors with more mesh replication, particularly in setup time, with reductions in total time per sweep (including pAIR setup and solve for all angles) reduced by 30-50% compared with no parallelism in angle. The pAIR setup times are shown in Figure 11.

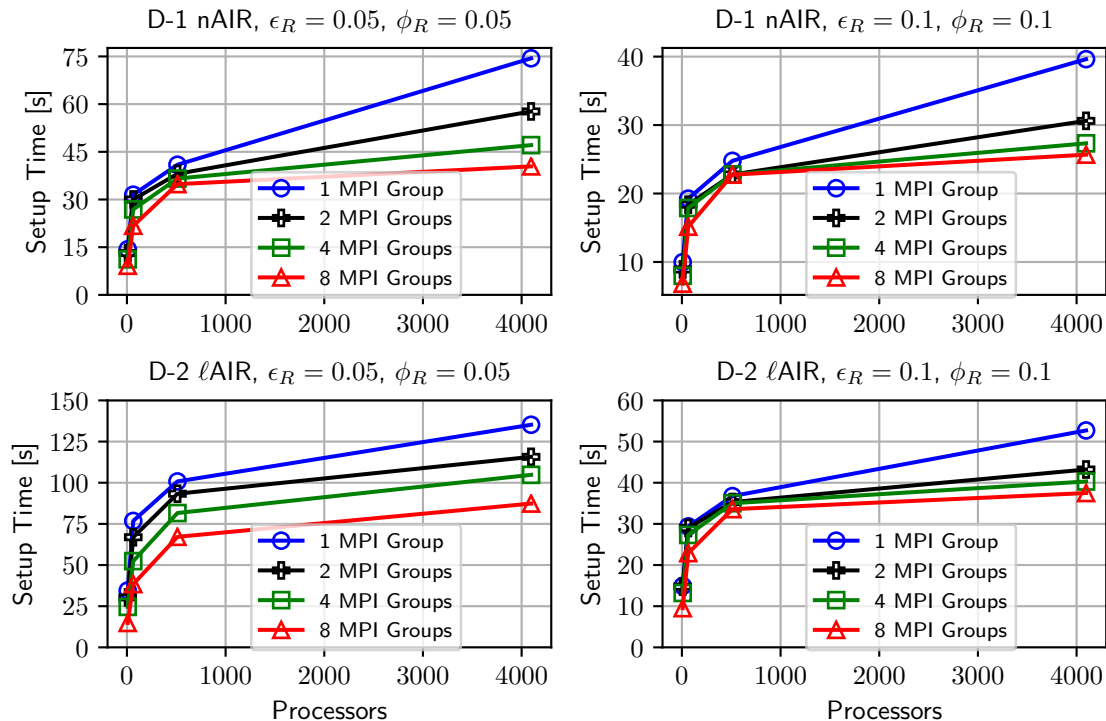


Fig. 11. AMG setup time and solve time shown for weak scaling with different numbers of replicated meshes. Results are shown for both  $\ell$ AIR and nAIR.  $\phi_R$  is the level of filtering on  $R$

The solve time and average convergence factor, for D-1 nAIR are shown in Figure 12. Results are only shown for nAIR because the solve time and CF of D1 nAIR and D-2  $\ell$ AIR are almost identical (in fact, the preconditioners are almost identical when applied to linear transport on a structured grid [3]). Here, the linear systems are solved to a relative tolerance of  $1e-6$  instead of to machine precision as in Section IV. Notice that the average convergence factors decrease

significantly with multiple meshes, due to the on-processor relaxation solving a larger part of the domain directly, but the solve times are more or less constant. In this case, the reduced communication and faster convergence is offset by the additional computation required when a larger portion of the spatial problem is stored on processor.

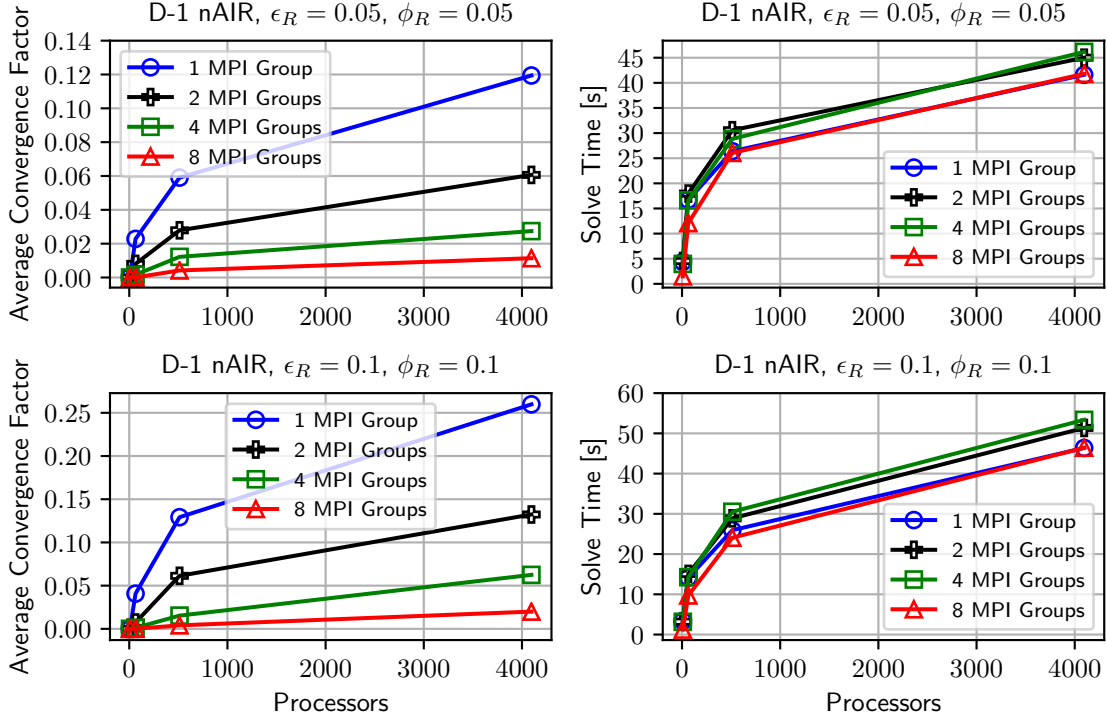


Fig. 12. Average convergence factors shown for weak scaling with different numbers of replicated meshes. Results are shown for both  $\ell$ AIR and nAIR

Although these results only consider the setup and solve time for a single sweep, they extend to the general time to solution of source iteration as well. The only overhead of parallel in angle vs. only spatial parallelism is additional communication to compute the scalar flux. However, communicating and computing the scalar flux is very cheap compared to angular flux calculations with pAIR. For example, with 8 MPI groups the computation and communication to form the scalar flux takes less than 1/10th of a second on 4096 processors, an insignificant amount of time compared to the reduction in time obtained through mesh replication. Thus, if multiple meshes reduce the total time for a single iteration by 30%, then total time of  $n$  source iterations will also decrease by  $\approx 30\%$ .

## VI. REPRESENTATIVE PARALLEL SWEEP RESULTS

As discussed in Section I.A, provably optimal methods have been developed for solving the  $S_N$  equations discretized on a structured mesh using parallel sweeps. These methods have been implemented in the deterministic transport program PDT [8, 23]. Figure 13 shows the time required by PDT to complete a full sweep of all 32 directions used in the three-dimensional problem with a uniform mesh described in Section IV. Results are presented for a hybrid KBA partitioning as well as a volumetric partitioning. The volumetric partitioning has better parallel scalability than

the hybrid KBA, but there is a larger constant associated with the scaling law [24] and so hybrid KBA is less costly for the problem investigated here.

When presenting scaling results, it is common and sensible to discuss relative times; however, actual solution times are presented in this section. The purpose of these results is not to investigate the scalability of parallel sweeps, as has been done in other works including [25], but to provide a representative result for the cost of parallel sweeps for comparison. The times presented depend on many factors besides the parallel algorithm including details of code implementation and computer characteristics.

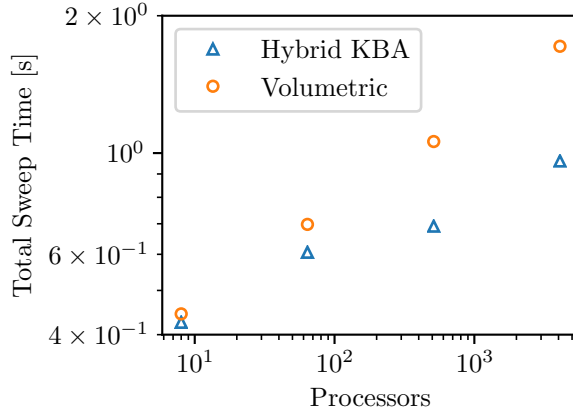


Fig. 13. Time taken for a single parallel sweep of 32 directions with PDT. Results are shown for both a hybrid KBA and volumetric cell partitioning

As discussed in Sections I.A and I.C parallel sweeps have poorer theoretical scaling compared to AMG, which has a logarithmic dependence on  $P$  rather than polynomial; however, these scaling laws say nothing about the constants associated with the growth in solution time. The constant associated with the AMG weak scaling law is generally much larger than that associated with parallel sweeps for a structured mesh. For the three-dimensional cube investigated here with a structured mesh, fitting a constant  $CP^{1/3}$  to the data in Figure 13 and extrapolating to large  $P$  predicts a crossover point where pAIR would out perform parallel sweeps on the order of 100 million processors.

Despite the large crossover point, it is worth pointing out that PDT is highly optimized and designed for uniform structured grids. These results will not be generally applicable to unstructured meshes. It is challenging to make a general statement regarding the efficiency of parallel sweeps on unstructured meshes. For example, a recent work has shown good scaling for parallel sweeps out to millions of MPI processes when there is some coarse regularity to an unstructured mesh such that it can be decomposed into well balanced regular partitions [26]. However, to our knowledge, no comparably scalable method has been demonstrated for a general unstructured mesh, even in the case where the mesh has no cycles. Furthermore, cycles in a mesh (in which case the resulting matrix is not triangular) require determining some ordering in which to sweep. In [27], a cycle-breaking strategy is developed for highly curved meshes. That strategy provides an important framework in which to sweep on very unstructured or curvilinear meshes, but source iteration was shown to converge in up to  $3\times$  less iterations when inverting the transport equations exactly with pAIR compared with sweeping and cycle breaking.

Conversely, pAIR is robust on arbitrary unstructured and curvilinear meshes, but optimization of pAIR is an ongoing process. Preliminary data suggests setup time of pAIR can be reduced significantly, and recent work on parallel sparse matrix operations [28, 29] shows that improved

communication algorithms can speed up the setup and solve phase by several times. Section III indicates that pAIR solves do not need to be performed to a high accuracy. If we consider time-dependent transport (easier to solve than steady state), only a few pAIR iterations should be necessary, which will further reduce pAIR solve time by several times. Combining superior performance on unstructured or curvilinear meshes, a reduction in iterations for the time-dependent setting, and the potential reduction in total pAIR time to solution by several times, a crossover point may be possible in the millions of processors for some problems.

## VII. CONCLUSION

In this paper, pAIR is shown to be effective and scalable for solving the source iteration equations of the  $S_N$  approximation to the transport equation. Section II.A demonstrates pAIR is capable of excellent convergence factors for a variety of meshes and material configurations, and scaling tests in Section IV show pAIR as currently implemented is capable of nearly ideal multigrid scaling.

When memory allows for some number of replicated meshes, Section V shows that a parallel in angle with mesh replication implementation can significantly increase performance. In a multiphysics code, using this multiple mesh scheme globally may not be possible. However in this situation, if there is excess memory and a relatively fast mesh partitioning algorithm is available, a separate replicated mesh partitioning might be constructed and used for the transport solve.

Because pAIR is an algebraic solver implemented in a popular linear algebra library, it can be easily interfaced as a black-box solver to other programs. As demonstrated here, a program capable of solving transport was created with a popular FEM library. In particular, no changes or special treatment were required when using the p4est domain decomposition library to distribute and refine the mesh, and AIR has proven effective on arbitrary unstructured and curvilinear meshes. This is not generally possible to do with parallel sweeps, which even on structured grids, require specialized communication scheduling logic that is integral with domain partitioning. Although the superior asymptotic scaling of pAIR over traditional sweeps appears insufficient for pAIR to overtake sweeps in performance, at least on meshes with moderate structure, the generality and non-intrusiveness of pAIR as a solver offers significant other advantages.

## APPENDIX

The MMS source,  $q_{mms}$ , for error tests in Section III is shown below, where  $\mu$ ,  $\eta$ , and  $\zeta$  are the direction cosines and  $L$  is the length the cube side.

$$\begin{aligned}
 q_{mms} &= \langle \mu, \eta, \zeta \rangle \cdot \left\langle \frac{\partial(\Phi\Psi)}{\partial x}, \frac{\partial(\Phi\Psi)}{\partial y}, \frac{\partial(\Phi\Psi)}{\partial z} \right\rangle - \frac{\sigma_s}{4\pi} \Phi + \sigma_t \Phi \Psi \\
 \Phi &= \sin\left(\frac{x\pi}{L}\right) \sin\left(\frac{y\pi}{L}\right) \sin\left(\frac{z\pi}{L}\right) \\
 \Psi &= \left(1 + 2\mu\left(x - \frac{L}{2}\right)\right) \left(1 + 2\eta\left(y - \frac{L}{2}\right)\right) \left(1 + 2\zeta\left(z - \frac{L}{2}\right)\right)
 \end{aligned}$$

*Proof of Theorem 1.* The proof consists of deriving a function  $S_{AMG}(K)$  that gives the total number of communication stages as a function of  $K$ , and proceeding to show that  $\frac{\partial S_{AMG}}{\partial K} < 0$  for  $K \leq \min\{P, ME\}$ . Thus, increasing  $K$  to the minimum of these values is guaranteed to reduce  $S_{AMG}$ . By Assumption 2 and the fact that we cannot have more partitions than processors  $P$ , we cannot pick  $K$  larger than the minimum of these values. If  $\frac{PC_P - NC_T ME}{C_a NC_T} < \min\{ME, P\}$ , then Constraint 1 forces us to pick  $K = \frac{PC_P - NC_T ME}{C_a NC_T}$ .

Consider a model of total communication stages when applying pAIR as a solver for the transport sweeps. AMG has two phases, the setup and solve phase, with a total number of communication stages given by

$$\xi \log_2 \left( \frac{P}{K} \right)^\alpha, \quad (9)$$

for  $\alpha \in [1, 2]$ . Optimal performance is given by  $\alpha = 1$  (the assumption of the theorem, but we stay general for purposes of the conjecture). Here,  $\xi$  is a constant that reflects the cost of the setup and solve of AMG compared with a sweep, and typically  $\alpha \in [1, 1.5]$ . Each partition must solve  $ME/K$  angles, so (9) is multiplied by  $ME/K$ .

In addition to sweeps, the scalar flux must be accumulated for each energy, and the scattering source must be computed over all energy groups. These steps are accomplished by computing the scalar flux available on each processor and summing across partitions so that all partitions have the scalar flux for the energies on that partition. Let  $\psi_{\ell, \nu}(\mathbf{x})$  represent the angular flux in direction  $\ell$  with energy  $\nu$ . Let  $\phi_\nu(\mathbf{x})$  be the scalar flux with energy  $\nu$ . Let  $w_\ell$  be the quadrature weight and let  $\sigma_{\nu, \nu'}$  be the scattering cross-section from energy group  $\nu'$  to energy group  $\nu$ . The accumulation of the scalar flux has the form

$$\phi_\nu(\mathbf{x}) = \sum_1^{K_A} \left( \sum_{\ell=1}^{M_1} w_\ell \psi_{\ell, \nu}(\mathbf{x}) \right),$$

where the second sum represents summation on each processor and the first sum is across the  $K$  partitions. Likewise, accumulation of the scattering term has the form

$$Q_\nu(\mathbf{x}) = \sum_1^{K_E} \left( \sum_{\nu'=1}^{E_1} \sigma_{(\nu, \nu')} \phi_{\nu'}(\mathbf{x}) \right).$$

This requires  $S_A = \log_2(K_A)$  stages to compute all the scalar fluxes for each energy and  $S_E = \log_2(K_E)$  stages to compute the scattering kernel. Combining with the communication for pAIR leads to a model of the form

$$\begin{aligned} S_{AMG} &= \xi \log_2 \left( \frac{P}{K} \right) \frac{ME}{K} + \zeta \log_2(K_E) + \zeta \log_2(K_A) \\ &= \xi \log_2 \left( \frac{P}{K} \right) \frac{ME}{K} + \zeta \log_2(K). \end{aligned}$$

Here, a constant  $\zeta$  is introduced to acknowledge that the summation stages require less communication than the pAIR stages. Thus, we expect that  $\zeta \ll \xi$ .<sup>a</sup>

Then,

$$\begin{aligned} \frac{\partial S_{AMG}}{\partial K} &= \frac{\zeta}{\ln(2)K} - \frac{\xi ME}{\ln(2)K^2} - \frac{\xi ME \log_2 \left( \frac{P}{K} \right)}{K^2} \\ &= \frac{1}{K^2} \left[ \frac{K\zeta}{\ln(2)} - \xi ME \left( \frac{1}{\ln(2)} + \log_2 \left( \frac{P}{K} \right) \right) \right]. \end{aligned} \quad (10)$$

Note that multiplying  $\frac{\partial S_{AMG}}{\partial K}$  by  $K^2$  does not change the sign of the slope or the zeros, so consider

---

<sup>a</sup>This could also be normalized, but we prefer to explicitly include some leading constant for each.

the interior term

$$\begin{aligned} \mathcal{G}_0(K) &:= \frac{\zeta}{\ln(2)}K - \frac{\xi ME}{\ln(2)} \left( 1 + \ln \left( \frac{P}{K} \right) \right), \\ \frac{\partial \mathcal{G}_0}{\partial K} &= \frac{\zeta}{\ln(2)} + \frac{\xi ME}{\ln(2)K}. \end{aligned} \tag{11}$$

Note that  $\mathcal{G}_0(1) < 0$  and  $\frac{\partial \mathcal{G}_0}{\partial K} > 0$  for  $K > 0$ . Thus there exists exactly one zero of  $\frac{\partial S_{AMG}}{\partial K}$  for  $K > 1$ . A closed form in terms of special functions is given in the following lemma.

**Lemma 1.** *For  $\alpha = 1$ , the single zero of  $\frac{\partial S_{AMG}}{\partial K}$  (10) is given by*

$$K_0 = \frac{\xi ME}{\zeta} W \left( \frac{e\zeta P}{\xi ME} \right),$$

where  $W(\cdot)$  denotes the Lambert  $W$ -function.

*Proof.* The proof proceeds by construction. Recall the identity of the Lambert  $W$ -function that  $\ln(W(x)) = \ln(x) - W(x)$  [30]. Let  $C = \frac{\xi ME}{\zeta}$  and observe

$$\begin{aligned} C + C \ln \left( \frac{P}{K_0} \right) &= C + C \ln(P) - C \ln(K_0) \\ &= C + C \ln(P) - C \ln \left( CW \left( \frac{eP}{C} \right) \right) \\ &= C + C \ln(P) - C \ln(C) - C \ln \left( \frac{eP}{C} \right) + CW \left( \frac{eP}{C} \right) \\ &= CW \left( \frac{eP}{C} \right) \\ &= K_0. \end{aligned}$$

Thus  $K_0$  satisfies the relation

$$K_0 = \frac{\xi ME}{\zeta} \left( 1 + \ln \left( \frac{P}{K} \right) \right),$$

Appealing to (11) completes the proof.  $\square$

We now have everything we need to prove the final result. Suppose  $P < ME$  and let  $K = P$ . Then from (11),

$$G_0(P) = \frac{\zeta P}{\ln(2)} - \frac{\xi ME}{\ln(2)} < 0.$$

Because  $G_0(1) < 0$  and  $\frac{\partial G_0}{\partial K} > 0$ , this implies that  $\frac{\partial S_{AMG}}{\partial K} < 0$  for  $K \in [1, \min\{P, ME\}] = [1, P]$ .

Now suppose  $P \geq ME$ . Appealing to Lemma 1, it is sufficient to show that the root  $K_0$  of  $\frac{\partial S_{AMG}}{\partial K}$  satisfies  $K_0 > \min\{P, ME\} = ME$ , which implies  $\frac{\partial S_{AMG}}{\partial K} < 0$  for  $K \in [1, \min\{P, ME\}] = [1, ME]$ . Recall that for real, positive values,  $W(x)$  is monotonically increasing [30], as well as the

definition of the Lambert  $W$ -function given by  $x = f^{-1}(xe^x) := W(x)$ . Then observe,

$$\begin{aligned}
P \geq ME &\implies \frac{P}{ME} \geq e^{\frac{\zeta}{\xi}-1}, \\
&\iff \frac{e\zeta P}{\xi ME} \geq \frac{\zeta}{\xi} e^{\frac{\zeta}{\xi}}, \\
&\implies W\left(\frac{e\zeta P}{\xi ME}\right) \geq W\left(\frac{\zeta}{\xi} e^{\frac{\zeta}{\xi}}\right), \\
&\iff W\left(\frac{e\zeta P}{\xi ME}\right) \geq \frac{\zeta}{\xi}, \\
&\implies K_0 \geq ME.
\end{aligned}$$

□

*Partial proof of Conjecture 1.* For  $\alpha \in (1, 2]$ ,  $S_{AMG}$  take the more general form

$$\begin{aligned}
S_{AMG} &= \xi \log_2 \left(\frac{P}{K}\right)^\alpha \frac{ME}{K} + \zeta \log_2(K), \\
\frac{\partial S_{AMG}}{\partial K} &= \frac{1}{K^2} \left[ \frac{K\zeta}{\ln(2)} - \xi ME \left( \frac{\alpha \log_2 \left(\frac{P}{K}\right)^{\alpha-1}}{\ln(2)} + \log_2 \left(\frac{P}{K}\right)^\alpha \right) \right].
\end{aligned}$$

As before, we multiply  $\frac{\partial S_{AMG}}{\partial K}$  by  $K^2$  and define the functional

$$\mathcal{G}(K) = \frac{\zeta}{\ln(2)} K - \xi ME \left( \frac{\alpha \log_2 \left(\frac{P}{K}\right)^{\alpha-1}}{\ln(2)} + \log_2 \left(\frac{P}{K}\right)^\alpha \right),$$

where

$$\frac{\partial \mathcal{G}}{\partial K} = \frac{\zeta}{\ln(2)} + \frac{\xi ME \alpha}{\ln(2) K} \left( \frac{(\alpha-1) \log_2 \left(\frac{P}{K}\right)^{\alpha-2}}{\ln(2)} + \log_2 \left(\frac{P}{K}\right)^\alpha \right).$$

We assume that  $K \in [1, P]$ , in which case  $P/K \geq 1$  and  $\log_2 \left(\frac{P}{K}\right) \geq 0$ . Because the remaining constants,  $\xi, \zeta, M$ , etc., are positive,  $\frac{\partial \mathcal{G}}{\partial K} > 0$  for  $K \in [1, P]$ . Suppose  $P \geq 2$ . Then it is clear for  $K = 1$ ,  $\frac{\partial S_{AMG}}{\partial K} < 0$ . Conversely, if we let  $K = P$ , the log-terms vanish and  $\frac{\partial S_{AMG}}{\partial K} > 0$ . Because  $\frac{\partial \mathcal{G}}{\partial K} > 0$  for  $K \in [1, P]$ , there exists exactly one zero of  $\frac{\partial S_{AMG}}{\partial K}$  over the interval  $K \in (1, P)$ .

Determining the root of  $\frac{\partial S_{AMG}}{\partial K}$  without explicit constants is not trivial. However, we can note that

$$\frac{\partial S_{AMG}}{\partial K}[P] = \frac{\zeta}{\ln(2)P} < \frac{1}{P}.$$

Moreover, note that

$$\frac{\partial^2 S_{AMG}}{\partial K^2} = \frac{\mathcal{G}'(K)}{K^2} - \frac{2\mathcal{G}(K)}{K^3}.$$

We will now show that if  $\alpha \in (1, 2)$ ,  $\frac{\partial^2 S_{AMG}}{\partial K^2} > 0$  over the range  $(1, P)$ , implying that  $S_{AMG}$  is concave up. The purpose of this is that if  $\frac{\partial S_{AMG}}{\partial K}[P] < \frac{1}{P}$ , and the slope of  $S_{AMG}$  is strictly increasing, then for moderate to large  $P$ ,

1. the root  $K_0$  of  $\frac{\partial S_{AMG}}{\partial K}$  is likely quite close to  $K = P$ , and
2. choosing  $K = \min\{P, ME\}$  results in at most a marginal increase in  $S_{AMG}$  over the optimal,  $K_{opt}$ .

Showing  $\frac{\partial^2 S_{AMG}}{\partial K^2} > 0$  is equivalent to showing  $K^3 \mathcal{G}'(K) > K^2 \mathcal{G}(K)$ . Plugging in and expanding, this is equivalent to proving

$$\frac{\zeta K}{\xi} \leq ME \left[ \frac{\alpha(\alpha-1)}{\ln(2)} \log_2 \left( \frac{P}{K} \right)^{\alpha-2} + 3\alpha \log_2 \left( \frac{P}{K} \right)^{\alpha-1} + 2 \ln(2) \log_2 \left( \frac{P}{K} \right)^\alpha \right].$$

Due to the constraints that  $K \leq \min\{P, ME\}$  and the fact that  $\zeta < \xi$ , it is sufficient to prove the interior term on the right is  $\geq 1$ . Let us make the change of variables  $K = P/2^\ell$ , for  $\ell > 0$ , encompassing the range  $K \in (0, P)$ . Then we need to show

$$\mathcal{H}_\alpha(\ell) := \frac{\alpha(\alpha-1)}{\ln(2)} \ell^{\alpha-2} + 3\alpha \ell^{\alpha-1} + 2 \ln(2) \ell^\alpha \geq 1.$$

for  $\ell > 0$  and  $\alpha \in (1, 2)$ . A second-derivative test confirms that  $\mathcal{H}_\alpha(\ell)$  is concave up for  $\alpha \in (1, 2)$  and further algebra confirms a single critical point of  $\mathcal{H}_\alpha$  for  $\alpha \in (1, 2)$  at

$$\ell_0 = \frac{3 - 3\alpha + \sqrt{\alpha^2 + 6\alpha - 7}}{4 \ln(2)},$$

where the minimum of  $\mathcal{H}_\alpha(\ell)$  occurs at  $\ell_0 \in (0, 0.248)$  for  $\alpha \in (1, 2)$ . Plugging  $\ell_0$  into  $\mathcal{H}_\alpha(\ell)$  and plotting as a function of  $\alpha \in (1, 2)$  confirms that  $\mathcal{H}_\alpha(\ell) \geq \mathcal{H}_\alpha(\ell_0) > 1$ .

Due to the additional practical constraint that  $K$  must be integer valued and divide the number of processors, there is strong evidence that for  $\alpha \in (1, 2)$ ,

$$K_{opt} = \min \left\{ P, ME, \frac{PC_P - NC_T ME}{C_a NC_T} \right\}.$$

□

## ACKNOWLEDGMENTS

This material is based upon work supported by the Department of Energy, National Nuclear Security Administration, under Award Number DE-NA0002376.

## REFERENCES

- [1] P. LESAIN and P. A. RAVIART, “On a Finite Element Method for Solving the Neutron Transport Equation,” *Publications mathématiques et informatique de Rennes*, , *S4* (1974) URL [http://www.numdam.org/item/PSMIR\\_1974\\_\\_\\_S4\\_A8\\_0](http://www.numdam.org/item/PSMIR_1974___S4_A8_0).
- [2] T. A. MANTEUFFEL, S. MUNZENMAIER, J. RUGE, and B. S. SOUTHWORTH, “Nonsymmetric reduction-based algebraic multigrid,” *SIAM J. Sci. Comput. (to appear)* (2019).
- [3] T. A. MANTEUFFEL, J. RUGE, and B. S. SOUTHWORTH, “Nonsymmetric Algebraic Multigrid Based on Local Approximate Ideal Restriction ( $\ell$ AIR),” *SIAM J. Sci. Comput.*, **40**, 6, A4105 (2018).



- [4] T. S. HAUT, P. G. MAGINOT, V. Z. TOMOV, B. S. SOUTHWORTH, T. A. BRUNNER, and T. S. BAILEY, “An Efficient Sweep-based Solver for the  $S_N$  Equations on High-Order Meshes,” *Nuclear Science and Engineering*, 1–14 (2019).
- [5] R. S. BAKER and K. R. KOCH, “An Sn Algorithm for the Massively Parallel CM-200 Computer,” *Nucl. Sci. Eng.*, **128** (1998); 10.13182/NSE98-1.
- [6] J. LIU, C. LIHUA, W. Q. LIN, G. CHUNYE, J. JIE, G. XINBIAO, L. SHENGGUO, Q. HU, and T. MASTERSON, “Parallel Sn Sweep Scheduling Algorithm on Unstructured Grids for Multi-group Time-Dependent Particle Transport Equations,” *Nuclear Science and Engineering*, **184**, 4, 527 (2016); 10.13182/NSE15-53., URL <https://doi.org/10.13182/NSE15-53>.
- [7] T. S. BAILEY and R. D. FALGOUT, “Analysis of Massively Parallel Discrete-Ordinates Transport Sweep Algorithms with Collisions (LLNL-CONF-407968),” (Oct 2008).
- [8] M. P. ADAMS, M. L. ADAMS, W. D. HAWKINS, T. SMITH, L. RAUCHWERGER, N. M. AMATO, T. S. BAILEY, and R. D. FALGOUT, “Provably Optimal Parallel Transport Sweeps on Regular Grids (LLNL-CONF-407968),” (2013).
- [9] R. FALGOUT, “An introduction to algebraic multigrid,” *Computing in Science & Engineering*, **8**, 6, 24 (2009); 10.1109/MCSE.2006.105.
- [10] R. D. FALGOUT and U. M. YANG, “hypre: A library of high performance preconditioners,” *European Conference on Parallel Processing*, **2331 LNCS**, PART 3, 632 (2002).
- [11] G. ALZETTA, D. ARNDT, W. BANGERTH, V. BODDU, B. BRANDS, D. DAVYDOV, R. GASSMOELLER, T. HEISTER, L. HELTAI, K. KORMANN, M. KRONBICHLER, M. MAIER, J.-P. PELTERET, B. TURCK SIN, and D. WELLS, “The deal.II Library, Version 9.0,” *Journal of Numerical Mathematics*, **26**, 4, 173 (2018); 10.1515/jnma-2018-0054.
- [12] C. BURSTEDDE, L. C. WILCOX, and O. GHATTAS, “p4est: Scalable Algorithms for Parallel Adaptive Mesh Refinement on Forests of Octrees,” *SIAM Journal on Scientific Computing*, **33**, 3, 1103 (2011); 10.1137/100791634.
- [13] M. A. HEROUX, R. A. BARTLETT, V. E. HOWLE, R. J. HOEKSTRA, J. J. HU, T. G. KOLDA, R. B. LEHOUCQ, K. R. LONG, R. P. PAWLOWSKI, E. T. PHIPPS, A. G. SALINGER, H. K. THORNQUIST, R. S. TUMINARO, J. M. WILLENBRING, A. WILLIAMS, and K. S. STANLEY, “An overview of the Trilinos project,” *ACM Trans. Math. Softw.*, **31**, 3, 397 (2005); <http://doi.acm.org/10.1145/1089014.1089021>.
- [14] M. SALA and M. HEROUX, “Robust Algebraic Preconditioners with IFPACK 3.0,” SAND-0662, Sandia National Laboratories (2005).
- [15] D. S. KERSHAW, “Differencing of the diffusion equation in Lagrangian hydrodynamics codes,” *J. Comput. Phys.*, **39**, 375 (1981).
- [16] J. WARSA, K. THOMPSON, and J. MOREL, “Improving the Efficiency of Simple Parallel  $S_N$  Algorithms with Krylov Iterative Methods,” *Transactions of the American Nuclear Society*, 449–451 (2003).
- [17] V. FABER and T. A. MANTEUFFEL, “A look at transport theory from the point of view of linear algebra,” *Transport theory, invariant imbedding, and integral equations (Santa Fe, NM)*, 37–61, Dekker, New York.
- [18] B. S. SOUTHWORTH, M. HOLEC, and T. S. HAUT, “Diffusion synthetic acceleration for heterogeneous domains, compatible with voids,” *Nuclear Science and Engineering* ((in review)).

- [19] W. WALTERS, “Use of the Chebyshev-Legendre quadrature set in discrete-ordinate codes,” Los Alamos National Lab., NM (1987).
- [20] T. A. MANTEUFFEL, L. N. OLSON, J. B. SCHRODER, and B. S. SOUTHWORTH, “A Root-node Based Algebraic Multigrid Method,” *SIAM Journal on Scientific Computing*, **39**, 5, S723 (2017).
- [21] M. R. DORR and C. H. STILL, “A concurrent, multigroup, discrete ordinates model of neutron transport,” *Proceedings of Scalable Parallel Libraries Conference*, IEEE (1993).
- [22] M. R. DORR and C. H. STILL, “Concurrent source iteration in the solution of three-dimensional, multigroup discrete ordinates neutron transport equations,” *Nuclear science and engineering*, **122**, 3, 287 (1996).
- [23] G. TANASE, A. BUSS, A. FIDEL, HARSHVARDHAN, I. PAPADOPOULOS, O. PEARCE, T. SMITH, N. THOMAS, X. XU, N. MOURAD, J. VU, M. BIANCO, N. M. AMATO, and L. RAUCHWERGER, “The STAPL Parallel Container Framework,” *SIGPLAN Not.*, **46**, 8, 235 (2011); 10.1145/2038037.1941586., URL <http://doi.acm.org/10.1145/2038037.1941586>.
- [24] S. D. PAUTZ and T. S. BAILEY, “Parallel Deterministic Transport Sweeps of Structured and Unstructured Meshes with Overloaded Mesh Decompositions,” *Nuclear Science and Engineering*, **185**, 1, 70 (2017); 10.13182/NSE16-34., URL <https://doi.org/10.13182/NSE16-34>.
- [25] W. HAWKINS, T. BAILEY, M. ADAMS, P. BROWN, A. KUNEN, M. ADAMS, T. SMITH, N. AMATO, and L. RAUCHWERGER, “Validation of full-domain massively parallel transport sweep algorithms,” *Transactions of the American Nuclear Society*, **111**, 699 (2014).
- [26] M. P. ADAMS, M. L. ADAMS, W. D. HAWKINS, T. SMITH, L. RAUCHWERGER, N. M. AMATO, T. S. BAILEY, R. D. FALGOUT, A. KUNEN, and P. BROWN, “Provably Optimal Parallel Transport Sweeps on Semi-Structured Grids,” *arXiv e-prints*, arXiv:1906.02950 (2019).
- [27] T. HAUT, P. MAGINOT, V. TOMOV, B. SOUTHWORTH, T. BRUNNER, and T. BAILEY, “An efficient sweep-based solver for the SN equations on high-order meshes,” *Nuclear Science and Engineering*, 1–14 (2019).
- [28] A. BIENZ, L. OLSON, and W. GROPP, “Reducing Communication in Algebraic Multigrid with Multi-step Node Aware Communication,” *arXiv preprint arXiv:1904.05838* (2019).
- [29] A. BIENZ, W. D. GROPP, and L. N. OLSON, “Node aware sparse matrix–vector multiplication,” *Journal of Parallel and Distributed Computing*, **130**, 166 (2019).
- [30] R. M. CORLESS, G. H. GONNET, D. E. HARE, D. J. JEFFREY, and D. E. KNUTH, “On the Lambert W-function,” *Advances in Computational mathematics*, **5**, 1, 329 (1996).